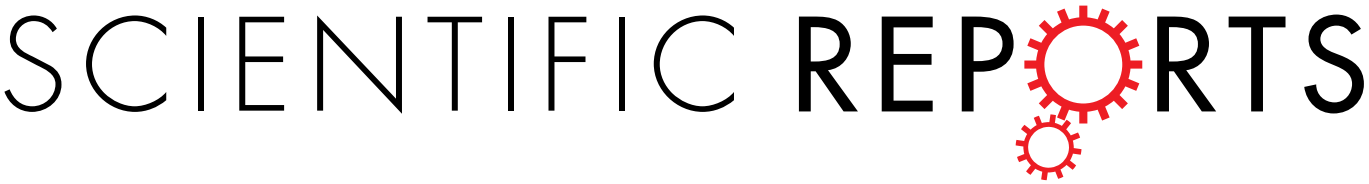

OPEN

Remote coral reefs can sustain high growth potential and may match future sea-level trends

Received: 12 October 2015
Accepted: 16 November 2015
Published: 16 December 2015

Chris T. Perry[1], Gary N. Murphy[1], Nicholas A. J. Graham[2,3], Shaun K. Wilson[4,5], Fraser A. Januchowski-Hartley[1] & Holly K. East[1]

Climate-induced disturbances are contributing to rapid, global-scale changes in coral reef ecology. As a consequence, reef carbonate budgets are declining, threatening reef growth potential and thus capacity to track rising sea-levels. Whether disturbed reefs can recover their growth potential and how rapidly, are thus critical research questions. Here we address these questions by measuring the carbonate budgets of 28 reefs across the Chagos Archipelago (Indian Ocean) which, while geographically remote and largely isolated from compounding human impacts, experienced severe (>90%) coral mortality during the 1998 warming event. Coral communities on most reefs recovered rapidly and we show that carbonate budgets in 2015 average +3.7 G (G = kg $CaCO_3$ m^{-2} yr^{-1}). Most significantly the production rates on *Acropora*-dominated reefs, the corals most severely impacted in 1998, averaged +8.4 G by 2015, comparable with estimates under pre-human (Holocene) disturbance conditions. These positive budgets are reflected in high reef growth rates (4.2 mm yr^{-1}) on *Acropora*-dominated reefs, demonstrating that carbonate budgets on these remote reefs have recovered rapidly from major climate-driven disturbances. Critically, these reefs retain the capacity to grow at rates exceeding measured regional mid-late Holocene and 20th century sea-level rise, and close to IPCC sea-level rise projections through to 2100.

Warming sea waters, ocean acidification and rising sea levels are effects of climate that pose a major threat to coral reefs globally[1,2]. At a local scale, reefs are also under ever-growing pressure from multiple direct human disturbances, including eutrophication and over-fishing, as well as disease outbreaks[3,4]. The net effect of these cumulative disturbances has been to fundamentally change reef ecology, with many reefs exhibiting reduced coral cover, altered coral and reef-associated species abundances, and diminished structural complexity[5–7]. On many disturbed reefs these changes are also now impacting the carbonate budgets of reefs[8], defined as the balance between the rate at which carbonate is produced by corals, coralline algal and other carbonate producing processes, set against the rate at which carbonate is either denuded by biological erosion ('bioerosion'), removed by physical processes, or chemically dissolved[9]. Where carbonate budgets are positive, reefs can maintain their physical three-dimensional structures and sustain high growth potential. However, under conditions of diminished production or increased bioerosion, carbonate budgets can become net negative, limiting reef growth and leading to reef structural collapse[10]. Such fundamental changes have now occurred across much of the Caribbean, where coral cover loss and community composition changes have caused both carbonate production and erosion rates to decline[11,12], significantly diminishing reef growth potential[8]. Similar trajectories are predicted for many reefs globally due to local disturbances and exacerbated by climate change[2,13,14].

Whilst many reefs have succumbed to the combined impacts of climate- and human-driven pressures, there remain regions largely free of direct human pressures due to their geographic remoteness. This raises the question of whether such reefs are better able to cope with global climate change impacts. The geographically isolated Chagos Archipelago, central Indian Ocean (Fig. 1), is one such region. It remains, with the exception of Diego Garcia, remote from direct human disturbance, and has fish populations that can be considered semi-pristine[15]. While the mass coral bleaching event of 1998 caused severe damage to reefs in Chagos, they have demonstrated

[1]Geography, College of Life and Environmental Sciences, University of Exeter, Exeter, UK. [2]Lancaster Environment Centre, Lancaster University, Lancaster LA1 4YQ, UK. [3]ARC Centre of Excellence for Coral Reef Studies, James Cook University, Townsville, QLD 4811, Australia. [4]Department of Parks and Wildlife, Kensington, Perth, Western Australia 6151, Australia. [5]School of Plant Biology, Oceans Institute, University of Western Australia, Crawley, Western Australia 6009, Australia. Correspondence and requests for materials should be addressed to C.T.P. (email: c.perry@exeter.ac.uk)

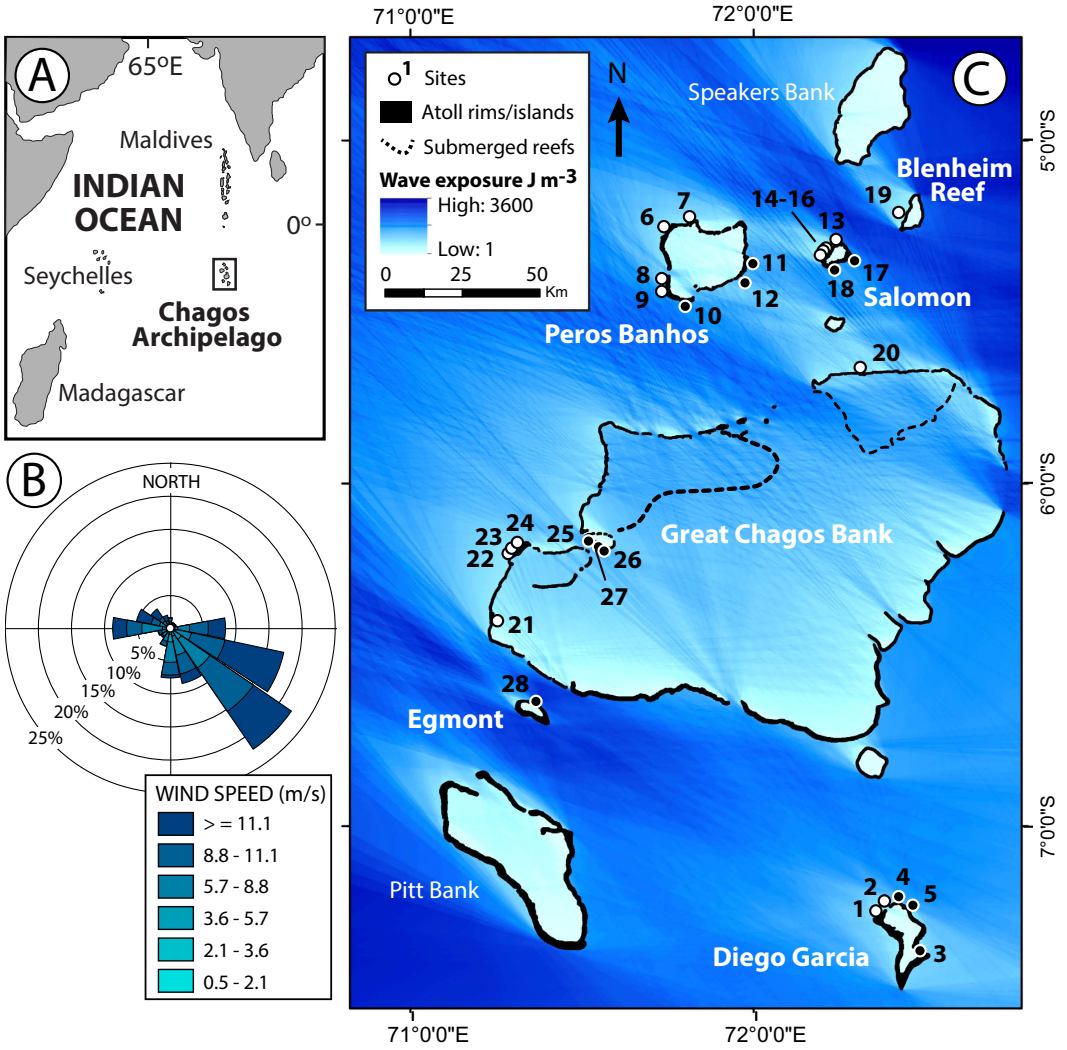

Figure 1. Study sites and wave energy regimes. (**A**) Location of the Chagos archipelago in the central Indian Ocean. Redrawn using Adobe Illustrator Version CS5 from Global and Planetary Change, Vol 82–83, R. P. Dunne *et al.* Contemporary sea level in the Chagos Archipelago, central Indian Ocean, p. 25–37, Copyright 2011, with permission from Elsevier; (**B**) Rose diagram showing the frequency and speed of winds (m s^{-1}) affecting Chagos plotted based on the direction from which winds are generated. Plots based on hourly wind measurements from 1973 to 2001 obtained from Diego Garcia airport (n = 219,943); (**C**) Major islanded atolls (bold white font) and submerged platforms of the Chagos Archipelago and modelled wave exposures (Joules m^{-3}). Numbered circles denote study sites, white fills are defined as 'sheltered' (<1000 J m^{-3}), black fills as 'exposed' sites (>1000 J m^{-3}): Diego Garcia - 1) Cannon Point, 2) Middle Island, 3) Horsborough Bay, 4) East Island, 5) Barton Point; Peros Banhos – 6) Ile Diamante, 7) Ile de la Passe, 8) Ile Poule, 9) Ile Gabrielle, 10) Ile Fouquet, 11) Grand Coquillage, 12) Petite Coquillage; Salomon – 13) Ile de Passe, 14) Ile Anglais north, 15) Ile Anglaise middle, 16) Ile Anglaise south, 17) Ile Takamaka, 18) Ile du Sel; Blenheim – 19) Blenheim west; Gt. Chagos Bank – 20) Nelson Island, 21) Danger Island, 22) Eagle Island south, 23) Eagle Island middle, 24) Eagle Island north, 25) Middle Brother, 26) South Brother west, 27) South Brother east; Egmont – 28) Egmont north east. Map generated in ArcMap 10.2.2 (www.esri.com/). Atoll outlines were imported into ArcMap from the Millennium Coral Reef Mapping Project (UNEP-WCMC), which is publicly available data on the web at the Institute for Marine Remote Sensing (University of South Florida) website (http://imars.usf.edu/MC/index.html). The dataset comprises 3 main components: (1) Millennium Coral Reef Mapping Project validated maps provided by the Institute for Marine Remote Sensing, University of South Florida (IMaRS/USF) and Institut de Recherche pour le Développement (IRD, Centre de Nouméa), with support from NASA; (2) Millennium Coral Reef Mapping Project unvalidated maps provided by the Institute for Marine Remote Sensing, University of South Florida (IMaRS/USF), with support from NASA. Unvalidated maps were further interpreted by UNEP-WCMC. Institut de Recherche pour le Développement (IRD, Centre de Nouméa) do not endorse these products; (3) Other data have been compiled from multiple sources by UNEP-WCMC and the WorldFish Centre in collaboration with WRI and TNC.

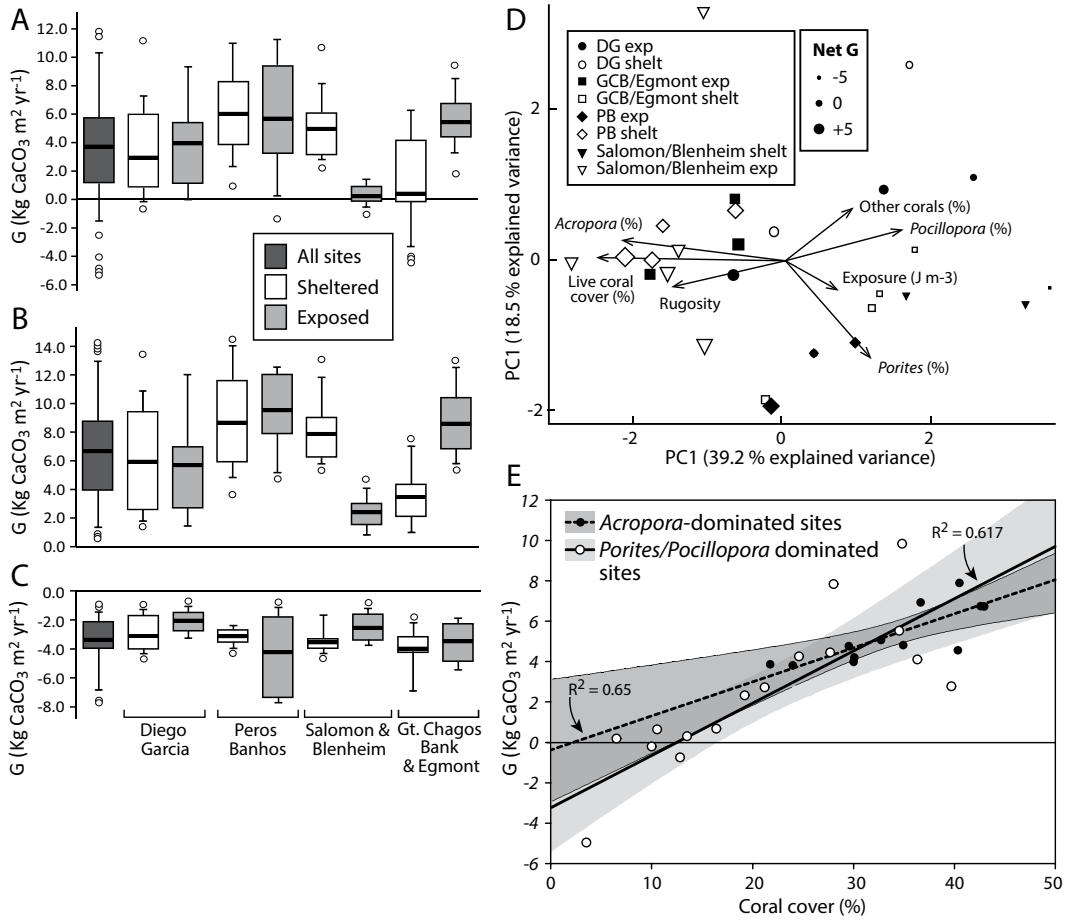

Figure 2. Net and gross carbonate production and erosion rates, and relationships to setting and exposure regime. Box (median and 50% quantile) and whisker (95% quantile) plots showing (**A**) net and (**B**) gross carbonate production rates, and (**C**) bioerosion rates for all sites and within each atoll. Atoll sites are grouped into "sheltered" and "exposed"; (**D**) Patterns in the net carbonate budgets of individual Chagos reefs assessed by correlation-based principle components analysis of $\log(x+1)$ transformed and normalized environmental data. Eigenvectors of each ecological and physical variable are overlaid; (**E**) The linear regression and 95% confidence interval for the relationship between coral cover and the net reef carbonate budget at sites across Chagos. Sites are differentiated into those that are either *Acropora*-dominated, or *Porites*/*Pocillopora*-dominated.

an impressive capacity for ecological recovery[16]. Here we use measured rates of both gross carbonate production and bioerosion from 28 reefs across 5 atolls in Chagos to determine their net biological carbonate budgets (G, where G = kg $CaCO_3 m^{-2} yr^{-1}$), and use these data to address two important questions: 1) have these reefs proved sufficiently resilient to recent climatic disturbances to regain rates of carbonate production and erosion that can be considered typical of undisturbed Indo-Pacific reefs? 2) do these reefs retain the capacity to accrete at rates sufficient to offset projected increases in sea level?

Results

Net carbonate production rates across all reefs averaged +3.7 G, with rates at the individual reef scale ranging from +9.8 to −5.0 G. Most reefs (25/28, 89%) had net positive budgets, and eight (29%) had budgets exceeding 5 G. Only 3 of the 28 reefs had net negative budgets (range: −0.3 to −5.0 G). There was, however, considerable heterogeneity in net G (Fig. 2A), with significant differences among reefs ($F_{24,82} = 8.584$, $p < 0.001$), although not among atolls ($F_{3,82} = 2.192$, $p = 0.113$). To explore the influence of wave exposure on carbonate budgets we compared averaged net and gross rates of production and erosion for sheltered and exposed reefs within each atoll, grouped based on wave energy regime. Average net G ranged from +0.2 to +6.0 G (Fig. 2A), with highest averages on reefs around both the 'sheltered' and 'exposed' margins of Peros Banhos (averages of +6.0 and +5.6 G respectively), from the 'sheltered' margin of Salomon (+5.0 G), and wave exposed sites on the Gt. Chagos Bank and Egmont (+5.4 G). Lowest net production rates were measured around the sheltered margins of Gt. Chagos Bank (+0.2 G) (Fig. 2A). Net G did not differ between sheltered and exposed sites within most atolls, the exception being the Gt. Chagos Bank, where exposed sites had significantly higher net G (atoll x exposure $F_{3,21} = 6.054$, $p = 0.004$).

The generally high and positive carbonate budgets are reflected in high rates of gross carbonate production (Fig. 2B) and bioerosion (Fig. 2C). Gross carbonate production averaged +6.6 G across all reefs, but differed significantly among reefs ($F_{24,82} = 7.165$, $p < 0.001$). Highest production rates were measured at Ile Poule on the sheltered

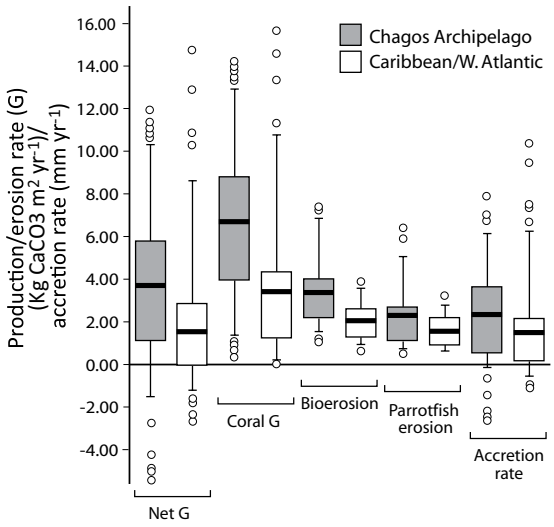

Figure 3. Comparisons between Chagos and the Caribbean. Box (median and 50% quantile) and whisker (95% quantile) plots showing regional differences in net G, coral G, bioerosion G, parrotfish G, and in accretion rates (mm yr^{-1}) between Chagos and the Caribbean. Caribbean data from Perry *et al.*[8,11,12].

margin of Peros Banhos (+11.2 G), and the lowest at Nelson at the northern margin of the Gt. Chagos Bank (+1.3 G), a reef with very low live coral cover (3.6%) as a result of recent (2015) Crown-of-Thorns starfish predation. Grouped- exposure/atoll average production ranged from +2.4 to +9.5 G (Fig. 2B), and significantly higher gross production rates were measured on the exposed compared to the sheltered Gt. Chagos Bank/Egmont reefs, while on Salomon production was significantly higher at the sheltered reefs (atoll x reef $F_{3,21} = 7.689$, $p = 0.001$). Bioerosion rates averaged 3.4 G across all reefs, with grouped-exposure/atoll averages ranging from −2.0 to −4.2 G (Fig. 2C), though bioerosion did not vary significantly with exposure ($F_{1,21} = 0.213$, $p = 0.673$). Bioerosion rates were significantly different between reefs ($F_{24,82} = 249.580$, $p < 0.001$), but not between atolls ($F_{3,82} = 1.212$, $p = 0.326$). Highest rates were measured at Petite Coquillage, Peros Banhos (7.4 G) and the lowest at East Island, Diego Garcia (1.4 G) (see Supplementary Table S1).

To understand which taxa are driving between-site variations in carbonate budgets we assessed net G as a function of coral taxa abundance, reef structure and exposure regime. As wave exposure increased the relative abundance of more robust taxa, but especially of *Porites* sp. and *Pocillopora* (mainly *P. eydouxi*), typically increased (Fig. 2D). These taxa thus dominate on most high wave exposure reefs (Fig. 1C), which generally have lower net G rates (Fig. 2D). In contrast, high net G rates are associated with sites defined by reduced wave exposure and an increased relative abundance of tabular and branched *Acropora* spp. (Fig. 2D). Whilst sites dominated by *Porites* spp. and *Pocillopora* spp. exhibit a wide range of net budget states, we note that high positive budgets are a defining feature of reefs where carbonate production is driven primarily by *Acropora* spp. (Fig. 2E). Furthermore, we note that whilst all *Acropora*-dominated sites are likely to retain net positive budgets unless coral cover falls below only a few %, that the transition into net negative states will occur at much higher coral cover levels where *Porites* and *Pocillopora* dominate (Fig. 2E), reflecting their lower calcification and extension rates[17].

Discussion

Our estimates of contemporary carbonate production and bioerosion across Chagos indicate that most reefs have responded positively to the climate-driven mortality of 1998 in terms of their carbonate budgets. The 1998 bleaching event resulted in the mortality of ~90% of corals down to ~15 m depth in the northern atolls, and to >40 m depth around Diego Garcia[18], a pattern repeated on many Indian Ocean reefs[19,20]. Shallow and mid-depth branching species, particularly *Acropora palifera* and table corals including *Acropora cytherea*, were especially impacted[21,22]. Since 1998, however, coral cover has recovered relatively rapidly at most sites and coral cover was restored to 1996 levels by 2010[23]. At the time of the present study (early 2015) we found that this coral recovery was reflected in generally high positive carbonate budgets on most reefs, with a third of surveyed reefs having net budgets in excess of 5 G. In addition, we note that our measured high coral production rates, which average around 6.9 G across sites, and especially those reported from the *Acropora*-dominated reefs (average 8.4 G), are close to the production rates (range ~5 to 9 G) reported as typical for undisturbed *Acropora*-dominated Indo-Pacific fore-reef settings[24]. Thus, whilst it is reasonable to assume that the 1998 event would have significantly diminished the budgets of most Chagos reefs, and especially those previously dominated by *Acropora* spp., contemporary rates have now recovered to be close to optimal for Indian Ocean reefs. This contrasts directly with the fundamental budget changes that persist at post-disturbance sites across the Caribbean, such that average carbonate production and erosion rates are higher (28% and 40% respectively) in Chagos relative to the Caribbean, and with particularly high coral production rates resulting in net G being twice as high compared to the Caribbean (Fig. 3).

We also note that on most reefs around Chagos carbonate production is predominantly driven by the same suite of coral genera; *Acropora*, *Porites* and *Pocillopora*, that dominated prior to the 1998 bleaching[22]. The relative

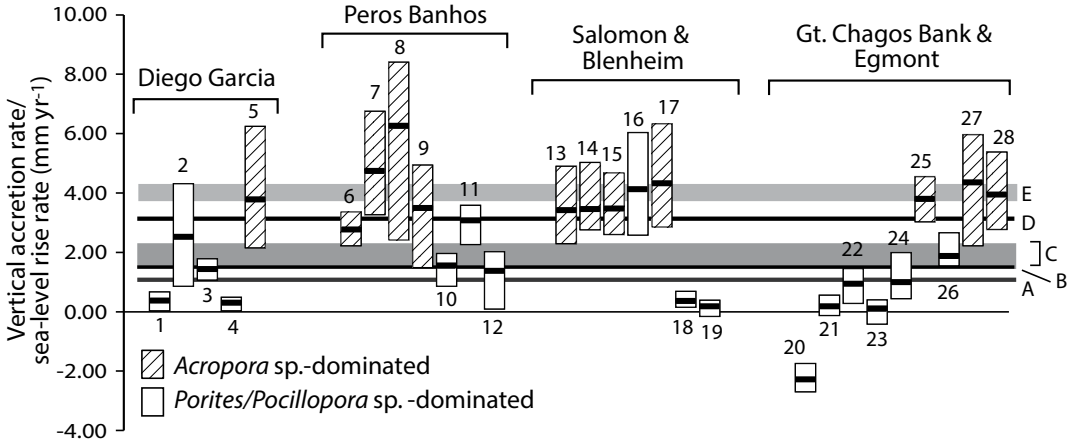

Figure 4. Reef accretion potential around Chagos and sea level trends and projections. Mean (black bar) and the maximum and minimum potential vertical accretion rates (mm yr^{-1}) for each site in Chagos (sites are ranked by increasing wave exposure within atolls), and shown relative to global and regional sea-level rise rates as follows: (**A**) Holocene trend from ~7,500 − 3,000 yBP[45]; (**B**) Average global rise rate over last 50 years (Church *et al.* 2013)[46]; (**C**) Range of measured rates around Chagos 1993 to 2011[43,44]; (**D**) Average global rise rate over last 20 years[35]; E. Average predicted rise rate for the central Indian Ocean by 2100 under RCP 4.5[35] and accounting for regional wind stress[35]. Site numbers as follows: 1. Cannon Pt, DG; 2. Middle Isld; DG, 3. Horsborough Bay, DG; 4. East Island, DG; 5. Barton Pt, DG; 6. Ile Diamante, PB; 7. Ile de la Passe, PB; 8. Ile Poule, PB; 9. Ile Gabrielle, PB; 10. Ile Fouquet, PB; 11. Grand Coquillage, PB; 12. Petite Coquillage, PB; 13. Ile Anglaise south, Sal; 14. Ile Anglaise middle, Sal; 15. Blenheim; 16. Ile Anglaise north, Sal; 17. Ile de Passe, Sal; 18. Ile du Sel, Sal; 19. Ile Takamaka, Sal; 20. Nelson, GCB; 21. Danger, GCB; 22. Eagle south, GCB; 23. Eagle middle, GCB; 24. Eagle north, GCB; 25. Egmont; 26. Middle Brother, GCB; 27. S. Brother west, GCB; 28. S. Brother east, GCB.

abundance of these genera differs among sites, largely as a function of exposure regime, but they collectively contribute >70% on average of the coral carbonate being produced. We thus find no evidence for the persistence of widespread coral community changes such as have occurred on reefs across the Caribbean, and at other less remote Indo-Pacific sites[25–27]. In the Caribbean these changes have resulted in shifts towards coral species that were not historically important framework builders[12], a change that has long-term implications for reef functionality because these "novel" community states may have a high probability of persisting into the future[28–30], and thus of locking reefs into lower carbonate budget states. However, whilst such transitions have not widely occurred on Chagos, ecological models predict any increase in extensive mortality events would have the capacity to drive such transitions[31]. It is thus pertinent to note the recent reports of partial mortality of colonies of *A. cytherea* at some Chagos sites[32], a fact noted in our own studies in 2015, and that some sites have also been impacted in recent years by COTS outbreaks[33]. Of most immediate concern however is the potential for another major bleaching-induced die-off, with the widespread bleaching reported during the mid-2015 sea-surface temperature anomaly event a clear indicator of the potential for such events to re-occur.

Arising from these observations are two important and inter-related questions about the maintenance of reef structures under future climate change. Firstly, what are the implications of the generally rapid coral community rebound around Chagos for reef growth potential? Secondly, what capacity does this instil in these reefs to respond positively to rising sea levels? Evidence from the Caribbean suggests that reef growth potential in that region has diminished, with accretion rates (mm yr^{-1}) an estimated order of magnitude lower than that measured in regional Holocene core records for equivalent depth assemblages[8]. In contrast, maximum potential accretion rates around Chagos average 2.3 mm yr^{-1} across all sites, but are higher (mean: 4.2 mm yr^{-1}) within *Acropora*-dominated sites, compared to *Porites*/*Pocillopora* dominated sites (mean: 0.9 mm yr^{-1}) (Fig. 4). Considerable between-site/atoll variability is also evident, with highest rates occurring on reefs along the sheltered margins of Peros Banhos (4.30 mm yr^{-1}) and Salomon (3.74 mm yr^{-1}), and on the Brothers reefs (Gt. Chagos Bank; 3.36 mm yr^{-1}) (Fig. 4). The lowest rates occur at those few sites (Nelson Island, and along the western margins of the Gt. Chagos Bank) where localised COTS outbreaks have caused recent coral mortality[33]. Viewed in the context of Indian Ocean Holocene reef growth, where shallow water accretion rates have averaged ~3.1 mm yr^{-1} over the last ~6,500 years[34], our datasets suggest that the current prognosis in terms of reef growth potential around Chagos, and especially for the *Acropora*-dominated reefs, is positive.

Predicting reef structural integrity and growth potential under present and future sea-level rise scenarios is more problematic and depends on the interaction between reef accretion potential (driven partly by reef ecology) and sea-level rise rates. A comparison of our accretion rate estimates against recent regional sea-level trends indicates that many Chagos reefs, including all those dominated by *Acropora* spp., should have the potential to accrete at rates above those measured using sea level altimetry data over the period 1950 to 2000 (Fig. 4). Projecting into the future, the IPCC AR5 report projects a global mean sea-level rise rate by 2081-2100 of a little above 4 mm yr^{-1} for the central Indian Ocean under scenario RCP 4.5[35], and accounting for regional wind-stress[36]. These rates are close to the average potential vertical accretion rates measured across our *Acropora* dominated sites (~4.2 mm yr^{-1}),

suggesting that even under these elevated rise rates that most *Acropora*-dominated reefs have the potential to closely track rising sea-levels over the coming century. However, higher rates predicted under RCP 6.0 and 8.5 scenarios would lead to a slight deepening (in the order of a few decimetres) over the fore-reef slope habitats by 2100.

There are, however, two important caveats that need consideration here. The first is that *Acropora* sp. tend to be highly susceptible to episodic disturbances[26,27] and, as noted, localised partial mortality has recently impacted colonies of *A. cytherea*[32]. Thus carbonate budgets (and resultant accretion rates) may be inherently more dynamic over time on reefs dominated by such corals, compared to those where *Porites* and *Pocillopora* spp. drive carbonate production. Long-term potential accretion rates may therefore not be so different between the two, especially where coral cover and thus carbonate production (see Fig. 3E), is high. However, an additional contributing factor will be the rate of physical removal of framework which will, to varying degrees, reduce reef accretion. There is little data with which to parameterise models of physical reef framework removal but, using data on background rates from the Maldives[38], albeit from a different reefal setting, a reasonable estimate is that along sheltered reef margins about 20% of annual framework produced may be lost (compared to >50% along exposed margins). Assuming similar attrition rates this would lower average accretion on *Acropora*-dominated reefs to ~2.9 mm yr^{-1} (range 2.3 to 4.5 mm yr^{-1}). Thus, even accounting for framework removal the best available estimates would suggest that most 'sheltered' reefs will retain the capacity, providing *Acropora* cover is maintained, to accrete at rates above those measured across the region over the last ~50–60 years, and within or close to the rates projected for the next 100 years (Fig. 4). In contrast, it seems reasonable to assume that a high proportion of the carbonate produced from the upper shelf areas along the exposed atoll margins will be removed by physical processes. Indeed, we note that all the exposed margin sites lack Holocene framework, suggesting a situation of long-term carbonate export dominance in these settings. However, we also note that this has not previously inhibited reef flat and reef island development on these high energy margins, and thus conclude that continued coral health and carbonate productivity along these exposed margins will remain essential for supplying rubble and sediment[39] to maintain these reef flats and islands.

Collectively, these findings highlight the capacity of the Chagos reefs, which are both geographically remote and isolated from compounding human impacts, to not only recover their ecological and geomorphic functions relatively rapidly following major past climate-driven perturbations, but also to retain the capacity to respond positively to future increases in sea level. Clear differences in accretion potential occur between sites, largely reflecting reef ecology and wave exposure regimes, but the highest accretion rates presently occur predominantly on those reefs where *Acropora*-drives carbonate production, and which are mostly along sheltered atoll margins. A key implication of this is that the capacity of reefs to track projected sea-level rise is generally lost (and certainly threatened) in the absence of *Acropora*, although we must assume, given the higher susceptibility of *Acropora* spp. to episodic disturbance, that the accretion potential of such reefs may inherently fluctuate over time. This raises an important note of warning in relation to any increase in the magnitude and frequency of disturbance events, since these would most likely preferentially impact those coral taxa with the highest growth rates[17], and which thus have the greatest capacity to maintain high reef accretion rates. The developing "third global bleaching event"[40] provides a clear indication of the immediacy of such threats. Actions aimed at reducing the effects of local disturbances on reefs are thus critical to provide any buffering for reefs from climate-change and to instil any capacity to maintain their accretion potential that so critically underpins the provisioning of most ecosystem services.

Methods

Surveys were conducted during March/April 2015 on 28 reefs across the five islanded atolls of the Chagos Archipelago (numbers of survey sites in brackets): Diego Garcia (5); Peros Banhos (7), Salomon (6), Great Chagos Bank (8), and Egmont (1), as well as at one site on the submerged Blenheim Reef (Fig. 1C). A seasonally-shifting wind regime, with the predominant wind direction being from the south-east (Fig. 1B), results in marked spatial variations in wave energy around Chagos. Our site selection strategy was driven by a desire to survey sites on both the more sheltered (the south-west, western and northern margins of the atolls, and those on the more exposed margins (the north-east, east and south-eastern margins), as well as integrating sites that had been the focus of earlier ecological surveys. To enable us to classify these sites on the basis of their wave exposure regime, spatially explicit estimations of wave exposure were modelled as a function of wind speed and direction, and fetch length (i.e. the distance over open ocean that wind can travel in a specific direction unobstructed by land or reefs) (see SI Methods). Based on these model outputs (Fig. 1C) we thus classify our sites into 'exposed' (>1000 J m^{-3}) or 'sheltered' (<1000 J m^{-3}), this division being based on a natural break in the rank order of the data across all sites. We refer to these groupings in the text for descriptive purposes.

To quantify gross carbonate production and erosion and thus to determine net carbonate budgets (G, where G = kg $CaCO_3$ m^2 yr^{-1}) we used a modified version of the Reef Budget[41] methodology (see SI Methods). At each site, surveys were conducted at a depth of 8–10 m i.e., a little above the upper shelf break, and with replicate transects established running parallel to the reef crest, with a spacing of ~5 m between transects. With only two exceptions we collected data along 4 replicate transects at each site (the exceptions being Middle Island (n = 5) and Cannon Point (n = 3) on Diego Garcia). At the same time these surveys allowed us to collect data on substrate composition and reef rugosity as a function of the 3-dimensional surface of the reefs (see SI Methods). Based on these data we define *Acropora* spp. dominated, and *Porites/Pocillopora* spp. dominated reefs as those where these taxa contribute to >50% of coral carbonate production. To test for differences in net and gross production and erosion between sites and atolls ANOVA tests were run with, where appropriate, a Tukey post-hoc test. Principal Component Analysis (PCA) was used to explore the relationships between reef carbonate production rates and reef ecology, physical structure and exposure regime.

To assess the accretion potential of reefs, and to explore their capacity to respond to future projected regional sea-level rise rates, we converted our net production rate estimates to potential accretion rates (mm yr^{-1}). We used an approach previously applied to Caribbean reefs[8] that accounts for both framework carbonate production and

sediment reincorporation from reef bioeroding taxa, but was modified to also factor for variations in accumulating framework porosity as a function of between-site variations in reef community composition[42] (see SI Methods). Resultant reef accretion rates were compared to recent rates of sea level rise based on satellite altimetry data from the central Indian Ocean region over the period 1950–2000[43] and 1950–2009[44] (see SI Methods). To compare contemporary reef accretion potential to future sea-level rise trajectories we used the IPCC AR5 report projections for the period 2081–2100[35], based on scenario RCP 4.5 but also accounting for the impacts of future wind-stress[36].

References

1. Hughes, T. P. *et al.* Climate change, human impacts, and the resilience of coral reefs. *Science* **301,** 929–933 (2003).
2. Hoegh-Guldberg, O. *et al.* Coral reefs under rapid climate change and ocean acidification. *Science* **318,1737**–1742 (2007).
3. Hughes, T. P. Catastrophes, phase shifts, and large-scale degradation of a Caribbean coral reef. *Science* **265,** 1547–1551 (2003).
4. Fabricius, K. E. Effects of terrestrial runoff on the ecology of corals and coral reefs: review and synthesis. *Marine Pollution Bulletin* **51,** 125–146 (2005).
5. Gardner, T. A., Côté, I. M., Gill, J. A., Grant, A. & Watkinson, A. R. Long-term region-wide declines in Caribbean corals. *Science* **301,** 958–960 (2003).
6. Alvarez-Filip, L., Dulvy, N. K., Gill, J. A., Côté, I. M. & Watkinson, A. R. Flattening of Caribbean coral reefs: region-wide declines in architectural complexity. *Proceedings of Royal Society B* **276,** 3019–3025 (2009).
7. Graham, N. A. J., Jennings, S., MacNeil, M. A., Mouillot, D. & Wilson, S. K. Predicting climate-driven regime shifts versus rebound potential in coral reefs. *Nature* **518,** 94–97 (2015).
8. Perry, C. T. *et al.* Caribbean-wide decline in carbonate production threatens coral reef growth. *Nature Communications*, doi: http://dx.doi.org/10.1038/ncomms2409 (2013).
9. Perry, C. T., Spencer, T. & Kench, P. Carbonate budgets and reef production states: a geomorphic perspective on the ecological phase-shift concept. *Coral Reefs* **27,** 853–866 (2008).
10. Eakin, C. Where have all the carbonates gone? A model comparison of calcium carbonate budgets before and after the 1982-1983 El Nino at Uva Island in the eastern Pacific. *Coral Reefs* **15,** 109–119 (1996).
11. Perry, C. T. *et al.* Changing dynamics of Caribbean reef carbonate budgets: emergence of reef bioeroders as critical controls on present and future reef growth potential. *Proceedings of the Royal Society B* **281,** 2014–2018 (2014).
12. Perry, C. T. *et al.* Regional-scale dominance of non-framework building corals on Caribbean reefs affects carbonate production and future reef growth. *Global Change Biology* **21,** 1153–1164 (2015).
13. Veron, J. E. N. *et al.* The coral reef crisis: The critical importance of <350 ppm CO_2. *Marine Pollution Bulletin* **58,** 1428–1436 (2009).
14. Kennedy, E. V. *et al.* Avoiding coral reef functional collapse requires combined local and global action. *Current Biology* **23,** 912–918 (2013).
15. Graham, N. A. J. & McClanahan, T. R. The last call for marine wilderness? *BioScience* **63,** 397–402 (2013).
16. Sheppard, C. R. C. *et al.* In coral reefs of the United Kingdom Overseas Territories, coral reefs of the World 4 (ed. Sheppard C. R. C.), Ch. 17, 241–253 (Springer, 2013) coral reefs of the Chagos Archipelago, Indian Ocean.
17. Pratchett, M. S. *et al.* Spatial, temporal and taxonomic variation in coral growth – implications for the structure and function of coral reef ecosystems. *Oceanography and Marine Biology: An Annual Review* **53,** 215–295 (2015).
18. Sheppard, C. R. C. Coral decline and weather patterns over 20 year in the Chagos archipelago, central Indian Ocean. *Ambio* **28,** 472–478 (1999).
19. Graham, N. A. J. *et al.* Climate warming, marine protected areas and the ocean-scale integrity of coral reef ecosystems. *PLoS One* **3,** e3039 (2008).
20. Ateweberhan, M., McClanahan, T. R., Graham, N. A. J. & Sheppard, C. R. C. Episodic heterogeneous decline and recovery of coral cover in the Indian Ocean. *Coral Reefs* **30,** 739–752 (2011).
21. Sheppard, C. R. C. Coral cover, zonation and diversity on reef slopes of Chagos atolls, and population structures of the major species. *Marine Ecology Progress Series* **2,** 193–205 (1980).
22. Sheppard, C. R. C. In *Ecology of the Chagos archipelago* (eds Sheppard, C. R. C. & Seaward, M. R. D.), Ch. 7, 91–100 (Linnean Society/Westburg, 1999), Changes in coral cover on reefs of Chagos over eighteen years.
23. Sheppard, C. R. C. *et al.* Reefs and islands of the Chagos archipelago, Indian Ocean: why it is the world's largest no-take marine protected area. *Aquatic Conservation: Marine and Freshwater Ecosystems* **22,** 232–261 (2012).
24. Vecsei, A. A new estimate of global reefal carbonate production including the fore-reefs. *Global and Planetary Change* **43,** 1–18 (2004).
25. Loya, Y. *et al.* Coral bleaching: the winners and the losers. *Ecology Letters* **4,** 122–131 (2001).
26. McClanahan, T. R., Baird, A. H., Marshall, P. A. & Toscano, M. A. Comparing bleaching and mortality responses of hard corals between southern Kenya and the Great Barrier Reef, Australia. *Marine Pollution Bulletin* **48,** 327–335 (2004).
27. Pratchett, M. S., McCowan, D., Maynard, J. A. & Heron, S. F. Changes in bleaching susceptibility among corals subject to ocean warming and recurrent bleaching in Moorea, French Polynesia. *PLoS One* **8,** e70443 (2013).
28. Côté, I. M. & Darling, E. S. Rethinking ecosystem resilience in the face of climate change. *PLoS Biol* **8,** e1000438 (2010).
29. Graham, N. A. J., Cinner, J. E., Norström, A. V. & Nyström, M. Coral reefs as novel ecosystems: embracing new futures. *Current Opinions in Environmental Sustainability* **7,** 9–14 (2014).
30. Yakob, L. & Mumby, P. J. Climate change induces demographic resistance to disease in novel coral assemblages. *Proceedings of National Academy of Science* **108,** 1967–1969 (2011).
31. Riegl, B., Sheppard, C. R. C. & Purkis, S. J. Human impact on atolls leads to coral loss and community homogenisation: a modelling study. *PLoS One* **7,** e36921 (2012).
32. Pratchett, M. S., Pisapia, C. & Sheppard, C. R. C. Background mortality rates for recovering populations of *Acropora cytherea* in the Chagos Archipelago, central Indian Ocean. *Marine Environmental Research* **86,** 29–34 (2013).
33. Roche, R. C. *et al.* Localized outbreaks of *Acanthaster planci* at an isolated and unpopulated reef atoll in the Chagos Archipelago. *Marine Biology* **162,** 1695–1704 (2015).
34. Montaggioni, L. F. History of Indo-Pacific coral reef systems since the last glaciation: development patterns and controlling factors. *Earth-Science Reviews* **71,** 1–75 (2005).
35. Church, J. A. *et al.* In *Climate Change 2013: The Physical Science Basis. Contribution of Working Group I to the Fifth Assessment Report of the Intergovernmental Panel on Climate Change.* (eds Stocker, T. F. *et al.*). Ch. 13, 1137–1216 (Cambridge University Press, 2013). Sea Level Change.
36. Timmermann, A., McGregor, S. & Jin, F. F. Wind effects on pastand future regional sea level trends in the southern Indo-Pacific. *Journal of Climate* **23,** 4429–4437 (2010).
37. McClanahan, T. R. *et al.* Western Indian Ocean coral communities: bleaching responses and susceptibility to extinction. *Marine Ecology Progress Series* **337,** 1–13 (2007).
38. Morgan, K. M. & Kench, P. S. A detrital sediment budget of a Maldivian reef platform. *Geomorphology* **222,** 122–131 (2014).
39. Perry, C. T., Kench, P. S., O'Leary, M. J., Morgan, K. M. & Januchowski-Hartley, F. Linking reef ecology to island-building: Parrotfish identified as major producers of island-building sediment in the Maldives. *Geology* **43,** 503–506 (2015).
40. Witze, A. Corals worldwide hit by bleaching (October 2015) (Date accessed: 19/10/2015) http://www.nature.com/news/corals-worldwide-hit-by-bleaching-1.18527

41. Perry, C. T. *et al.* Estimating rates of biologically driven coral reef framework production and erosion: a new census-based carbonate budget methodology and applications to the reefs of Bonaire. *Coral Reefs* **31,** 853–868 (2012).
42. Kinsey, D. W. & Hopley, D. The significance of coral reefs as global carbon sink-response to greenhouse. *Palaeogeography, Palaeoclimatology, Palaeoecology* **89,** 363–377 (1991).
43. Palanisamya, H. *et al.* Regional sea level variability, total relative sea level rise and its impacts on islands and coastal zones of Indian Ocean over the last sixty years. *Global and Planetary Change* **116,** 54–67 (2014).
44. Dunne, R. P., Barbosa, S. M. & Woodworth, P. L. Contemporary sea level in the Chagos Archipelago, central Indian Ocean. *Global and Planetary Change* **82-83,** 25–37 (2012).
45. Camoin, G. F., Montaggioni, L. F. & Braithwaite C. J. R. Late glacial to post glacial sea levels in the Western Indian Ocean. *Marine Geology* **206,** 119–146 (2004).
46. Church, J. A., White, N. J. & Hunter, J. R. Sea-level rise at tropical Pacific and Indian Ocean islands. *Global and Planetary Change* **53,** 155–168 (2006).

Acknowledgements

Field research was supported by DEFRA Darwin Initiative grant 19-027, 'Darwin Initiative to strengthen the world's largest Marine Protected Area, Chagos Archipelago', and John Turner (Bangor) and Charles Sheppard (Warwick) are thanked for coordinating the 2015 research cruise. NAJG was additionally supported by Australian Research Council grant DE130101705, FAJ-H through an Ecosystem Services for Poverty Alleviation (ESPA) grant 'Sustainable Poverty Alleviation from Coastal Ecosystem Services (SPACES)' (project NE-K010484-1), and HKE by Natural Environment Research Council Studentship NE/K500902/1 . We acknowledgement the invaluable support of The Chagos Conservation Trust, the Foreign and Commonwealth Office BIOT section, and the Captain and crew of the MV Pacific Marlin. Philip Woodworth (Southampton) is thanked for discussions on past sea-level trends.

Author Contributions

C.T.P. initiated the study, collected and analysed the field data. G.M., N.A.J.G. and S.K.W. helped collect and analyse the field data. F.A.J.-H. contributed to field methodology development. H.E. developed the wave exposure model. All authors contributed to manuscript writing.

Additional Information

Supplementary information accompanies this paper at http://www.nature.com/srep

Competing financial interests: The authors declare no competing financial interests.

How to cite this article: Perry, C. T. *et al.* Remote coral reefs can sustain high growth potential and may match future sea-level trends. *Sci. Rep.* **5**, 18289; doi: 10.1038/srep18289 (2015).

Supplementary methods and tables

Remote coral reefs can sustain high growth potential and may match future sea-level trends

Chris T. Perry[1*], Gary N. Murphy[1], Nicholas A.J. Graham[2,3], Shaun K. Wilson[4,5], Fraser A. Januchowski-Hartley[1], Holly K. East[1]

[1] Geography, College of Life and Environmental Sciences, University of Exeter, Exeter, U.K.

[2] Lancaster Environment Centre, Lancaster University, Lancaster LA1 4YQ, UK

[3] ARC Centre of Excellence for Coral Reef Studies, James Cook University, Townsville, QLD 4811, Australia

[4] Department of Parks and Wildlife, Kensington, Perth, Western Australia 6151, Australia.

[5] School of Plant Biology, Oceans Institute, University of Western Australia, Crawley, Western Australia 6009, Australia

*Corresponding author: c.perry@exeter.ac.uk

Supplementary methods

1. Study area

The Chagos archipelago is located in the central Indian Ocean (Lat: 5-7^{o}S, Long: 71-73^{o}E; and comprises five main atolls (see main Fig. 1C): Great Chagos Bank (~18,000 km^2) which is mostly submerged, but which has eight reef islands developed on its western and northern rims, Peros Banhos (~463 km^2) which has 24 reef islands around its rim, Salomon (~38 km^2) with 8 rim islands; Egmont (~40 km^2) with 2-3 islands on its rim (several islands having merged over the last decade or so), and Diego Garcia (~200 km^2) which has only 4 individual islands, but has the largest land area (2,733 ha) of any of the atolls. There are, in addition, a further ten submerged atolls and banks. Most islanded atolls have now been uninhabited for nearly 40 years, and thus the Chagos reefs are almost entirely free of direct anthropogenic impacts. Exceptions include the impacts of low (though poorly quantified) levels of illegal fishing on the outer atolls, impacts from recreational fishing around Diego Garcia (which has lower fish biomass than the other atolls [1]), and the effects of the terrestrial military development on Diego Garcia. The Chagos reefs are thus amongst the remotest in the Indo-Pacific and, in April 2010, the entire archipelago and its associated exclusive economic zone (an area of ~640,000 km^2) was officially established as a no-take marine protected area. Impacts linked to climatic change and to broad scale oceanic and meteorological disturbances thus currently represent the only serious threats to reef health and ecosystem function.

Our ecological and carbonate budget surveys were conducted during March to April 2015 on 28 reefs across each of the five islanded atolls (numbers of survey sites in brackets): Diego Garcia (5); Peros Banhos (7), Salomon (6), Great Chagos Bank (8), and Egmont (1), as well as at one site on the submerged Blenheim Reef (see main Fig. 1C). The atolls and platforms of Chagos are characterised by marked differences in wave energy regimes around their margins (see main Fig. 1C), driven by the seasonally-shifting wind regime, with the predominant wind direction being from the south-east (see main Fig. 1B). Our site selection strategy around atolls was driven by a desire to survey sites on both the more sheltered (the south-west, western and northern margins of the atolls, and those on the more exposed margins (the north-east, east and south-eastern margins), as well as integrating sites that had been the focus of earlier ecological surveys. At each site, surveys were conducted at a depth of ~10 m i.e., a little above the upper shelf break, and with replicate transects established running parallel to the reef crest, with a spacing of ~5 m between transects. With only two exceptions we collected data along 4 replicate transects at each site (the exceptions being Middle Island (n = 5) and Cannon Point (n = 3) on Diego Garcia).

2. Wave exposure modelling

To enable us to classify these sites on the basis of their wave exposure regime, spatially explicit estimations of wave exposure were modelled as a function of wind speed and direction, and fetch length (i.e. the distance over open ocean that wind can travel in a specific direction unobstructed by land or reefs). To do this we followed the same protocols previously applied in reef environments [2,3]. Fetch lengths were calculated using the USGS model[4] which uses the procedure recommended by the Shoreline Protection Manual[5]. A binary raster representing the distribution of land masses and reef crests was generated using the outputs of the Millennium Coral Reef Mapping Project at a spatial resolution of 30 m^2 [ref. 6]. Fetch lengths were generated for 16 compass directions (every 22.5^{0}) by calculating the arithmetic mean of 5 radials spread at 3^{0} increments around the desired wind directions. 650 km was used as a maximum limit for fetch length as this is the distance required for maximal wave conditions[7]. Hourly wind measurements from 1973 to 2001 were obtained from Diego Garcia airport (n = 219,943) and used to calculate both the probability of wind blowing from each of the 16 compass directions and also the mean velocities for each direction. Fetch lengths were then converted into wave energies based on linear wave theory and using established equations [ref2]. Based on model outputs (see main Fig. 1C) we have classified our sites into “exposed” (>1000 J m^{-3}) or “sheltered” (<1000 J m^{-3}), this division

being based on a natural break in the rank order of the data across all sites. We refer to these groupings in the text for descriptive purposes.

3. Quantifying carbonate production and erosion rates

To quantify gross carbonate production and erosion and thus to determine net carbonate production (G, where G = kg $CaCO_3$ m^2 yr^{-1}) we used a version of the ReefBudget methodology of Perry et al.[ref8] adapted and parameterised for the Indian Ocean. However, there are some importance differences: carbonate production by corals and coralline algae is calculated using geometric relationships derived from individual colony morphology, rather than calculated using rugosity at the level of the transect; and clinoid sponge bioerosion is calculated using published rates and the proportion of hard substrate under the transect line available for erosion. Sediment production by macro-bioeroders (urchins and parrotfish) is also estimated, but other aspects of sediment production and post-depositional lithification are not. Within each site, two different sets of transects were conducted, one set to census benthic carbonate producers and bioeroders, and one set to quantify parrotfish abundance and size.

Along each benthic assessment transect we measured the distance within each linear 1 m covered by each category of benthic cover beneath a 10 m guide line using a separate flexible tape. All overhangs, vertical surfaces and horizontal surfaces below the line were surveyed (i.e., if the guide line crossed over a table coral, the upper and lower surfaces of the coral, plus the benthos under the canopy, were recorded). The following groups were recorded: scleractinian corals to the genera and morphological level (e.g., *Acropora* branching, *Porites* massive etc.); crustose coralline algae (CCA) including CCA below macroalgal or soft coral cover; turf algae; fleshy macroalgae; non encrusting coralline algae (e.g., *Halimeda* sp., articulated coralline algae); sediment; bare substrate (e.g., granitic rock, limestone pavement); sediment; rubble; and other benthic organisms. Substrate rugosity was calculated as total reef surface divided by linear distance (a completely flat surface would therefore have a rugosity of 1).

3.1 Calculating carbonate production

In contrast to the original Reefbudget approach[8], we used the morphology and size of individual coral colonies in combination with genera specific skeletal density (g cm^{-3}) and linear growth rates (cm $year^{-1}$) across each transect to estimates carbonate production rates in kg $CaCO_3$ m^{-2} $year^{-1}$ (where m^2 refers to the planar surface of the reef). Where possible, we used published growth rates and skeletal densities from the Western/Central Indian Ocean, but when these were not available means of published growth rates and densities for each coral genera were used instead. These data were then combined with geometric transformations based on colony morphology to give a growth rate for each colony for the area under the transect line (taking a transect line width of 1cm): massive colonies were assumed to be hemispherical in cross-section; encrusting, foliose and plating colonies, as well as colonies of crustose coralline algae (CCA) were assumed to be growing primarily at the edge of the colony (and at 10% of this growth rate across the remainder of the colony); for branching colonies, the proportion of the colony area of growing branch tips was assumed to be growing at published rates, and the remainder of the colony at 10% of these rates. The equations used in our calculations are thus as follow:

Massive:

$$CP_i = \left(\left(g + \left(\frac{x}{\pi}\right)\right)^2 \pi - \left(\frac{x}{\pi}\right)^2 \pi\right).d$$

Encrusting etc.:

$$CP_i = 2(g.d) + 0.1g.x.d$$

Branching/corymbose etc.:

$$CP_i = (r.c_a.g.d) + (x - c_a.x).0.1g.d$$

Where CP_i = carbonate production for colony *i*, *g* = growth rate, *x* = surface length of colony, *d* = skeletal density and c_a = proportion of colony that are growing axial branches.

Measuring the linear surface of growing tips on branching corals is time-consuming. Therefore, in order to calculate the amount of each colony growing as axial branch tips, we used data previously obtained on the size of branching colonies and the length of growing tips from 405 coral colonies in northern Mozambique (293 *Acropora*, 62 *Pocillopora*, 26 *Porites*, 24 other) (ref. 9). We conducted linear regressions between colony size and length of growing tips for each genera/morphology combination for which we had greater than 20 replicates in order to calculate c_a. To calculate the production for a single transect over a year, the following equation was used:

$$CP_j = \sum_{i=1}^{n} CP_1 + CP_2 + \cdots + CP_n$$

Where CP_j is the total carbonate production of both corals and crustose coralline algae for transect *j* in kg $CaCO_3$ $year^{-1}$. To estimate the production rate of the reef, we then used the following equation:

$$Gprod_j = CP_j / (\frac{10000}{l})$$

Where $Gprod_j$ is the carbonate production rate of both corals and crustose coralline algae for transect *j* in kg $CaCO_3$ m^{-2} $year^{-1}$, and l is the transect length in centimetres.

3.2 Calcuating reef framework bioerosion

3.2.1. Micro- (endolithic) and Macro- (clionaid sponge, polychaetes, bivalves etc.) bioerosion

In general, macro-borer communities are less well-characterised in the Indo-Pacific than in the Caribbean. This is particularly true of clionaid sponges, which are generally cryptic and difficult to identify in the field, particularly for a non-expert, and are typically a less dominant part of the macroborer community than in the Caribbean. To this end, instead of conducting an intensive search of the substrate for clionaid sponges as described in Perry et al., (2012), we instead utilized published rates of total macrobioerosion measured at Indo-Pacific sites, alongside a census of substrate available for bioerosion from the benthic line-intercept transects. This comprises of all dead carbonate substrate available to bioeroding sponges, including that covered by macroalgae or algal turf and live coral cover and soft corals. While both live and soft corals can prevent settlement of most bioeroding sponges, live corals are often colonised by other bioeroders (particularly polychaete worms), while soft corals are often ephemeral, and removal of soft coral cover, either by predation or storms could allow settlement and establishment of bioeroders prior to regrowth. All substrate not available to bioeroders was excluded, and the following equation used:

$$\text{Microbioerosion} = S^*R^*E_m$$

$$\text{Macrobioerosion} = S^*R^*E_a$$

Where *S* is the percentage of surface area of the transect available for erosion, *R* is the rugosity of the transect, E_m is the erosion rate of microborers, and E_a is the erosion rate of macroborers in kg m^{-2} yr^{-1}.

3.2.2 Urchin bioerosion

The main agents of echinoid bioerosion on reefs belong the family Diadematidae, (*Diadema* spp., and *Echinothrix* spp.) and the genera *Echinometra*, *Echinostrephus* and *Eucidaris*. We censused urchin abundance, size and species composition within 10 x 2 m belt transects along the main benthic transect lines at each site. These census data were then combined with carbonate ingestion rates from the literature and adjusted to account for the rugosity of the substrate. A variety of techniques have been used to estimate bioerosion rates in these urchin species: including $CaCO_3$ content of the gut (e.g., ref. 10) or of their faecal pellets (e.g., ref. 11), both with or without estimations of reworked sediment, spine abrasion and gut turnover (e.g., ref. 12, 13). This makes it difficult to compare bioerosion rates derived from different studies. However, evaluating the published data on erosion rates against test size across all urchin species suggest a relatively tightly correlated plot. SI Figure 1A shows the pooled bioerosion rates relative to test size for six species of urchins across 10 studies in the Indian and Pacific Oceans, with SI Figure 1B showing the rates for *Echinometra mathaei* and the *Diadematidae*. This allows us to calculate the erosion rate (kg urchin^{-1} year^{-1}) for each individual urchin using one of the following equations:

Diadematidae bioerosion (B_D) = $(0.000001*x^{3.4192})*0.365$

Echinometra mathaei bioerosion (B_E) = $(0.0004*x^{1.9786})*0.365$

General equation for all other bioeroding species (B_G) = $(0.0001*x^{2.323})*0.365$

To calculate bioerosion by urchins in kg m^{-2} year^{-1}, we summed the erosion rates of all individual urchins within each transect (U_E), and divided by the surface areas within each transect which was calculated as planar surface area (usually 20 m^2) multiplied by rugosity.

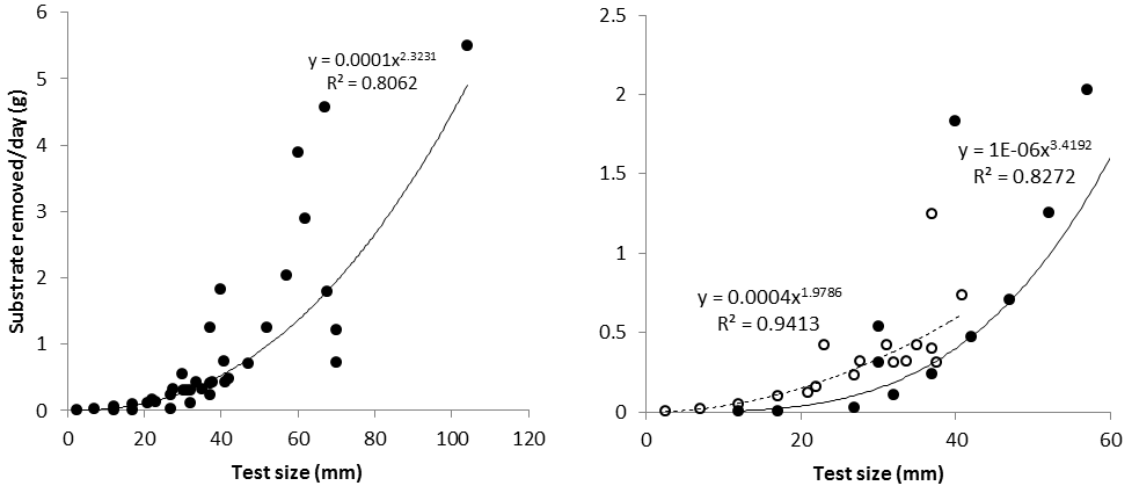

SI Figure 1 *(A) Bioerosion rates (substrate removed/day (g)) for urchins across a range of test size (Indo-Pacific data only). Data aggregated from: ref. 10, 14 – 21. (B) Bioerosion rates for Diadematidae (closed circles) and Echinometra metra (open circles).*

3.2.3. Parrotfish bioerosion

To determine the species-size-life phase abundances of bioeroding parrotfish at each site we used underwater census data for Chagos collected in 2010 and 2012[ref. 22], augmented by additional data collected in 2015. At each site four 50 m x 5 m belt transects were used (covering 1000 m^2 of reef). Time to complete transects was not held constant but adjusted according to the numbers of fish in the sampled areas. All fish surveys were completed by the same experienced observers (N.A.J.G., S.K.W or G.N.M). Biomass of individual fish was then calculated using estimated length data and length-weight relationships [23,24]) and multiplying by abundance of the species or family of the fish. To calculate parrotfish bioerosion rates by each individual fish we then used a

model based on total length and life phase to predict the bite rates (bites hr^{-1}) for each species. For species for which data was not previously available, we have made use of new observations)[9] or have used data from similar sized species with the same feeding functional group. Daily bite numbers were calculated using diurnal feeding activity reported in Bellwood[25]. Bite volume data has been obtained from published studies [25,26]. Where no bite volume data exists, we have either measured the size of individual bites *in situ* using Vernier callipers to obtain width and length of bite, or obtained from published studies estimates of bite area (e.g., Ref 27). We have then used a bite depth of 0.1 mm to obtain a conservative estimate of bite volume for *Scarus* sp. Not all bites on the substratum remove material and we have assumed, following Bellwood & Choat[28], that only bites that leave visible scars are eroding the substrate. In order to estimate the proportion of bites resulting in scars on the substratum for each size class, we extrapolated from published literature [26,29] and used the same method as above where data was missing. We used the following equation to calculate species specific erosion rates for the median value within each size class:

$$\text{Bioerosion rate (kg.ind}^{-1}\text{yr}^{-1}) = v.s_{prop}.br.d*365$$

Where v is bite volume (cm^3), s_{prop} is the proportion of bites leaving scars, b_r is bite rate (bites day^{-1}) and d is substratum density (kg cm^{-3}), here taken to be $1.49*10^{-3}$

4. Statistical treatment of data

Variation in bioerosion, and in net and gross production of carbonate, were analysed with respect to reef, atoll and exposure using analysis of variance, where reef was nested within atoll. Data were plotted and tested for normality and homogeneity of variance prior to analyses and transformed to meet these assumptions when appropriate. Significant results were further investigated with a post-hoc Tukey test. The interaction between atoll and exposure was investigated by pooling data at the reef level. Differences in the influence of different variables on net carbonate budgets between reefs were examined using correlation-based principle components analysis (PCA). Data were log(x + 1) transformed and normalized to account for skewness and to ensure all metrics were on a common scale. We overlaid eigenvectors to identify the direction and contribution of different variables to the patterns. The PCA was conducted using the prcomp function in R 3.1.1.

5. Reef accretion rates and comparisons to recent and future sea level trends

To assess the accretion potential of reefs, and to explore their capacity to respond to future projected regional sea-level rise rates, we converted our net production rate estimates to potential accretion rates (mm yr^{-1}). To do this we used an approach previously applied to Caribbean reefs [30], but modified to also factor for variations in accumulating framework porosity as a function of between-site variations in reef community composition. Specifically, we estimated the maximum accretion potential of each reef as a function of the net carbonate production rate of the site (calculated as gross production less gross erosion rate) and assumed that a proportion of the bioeroded framework (that is converted to sediment) is also reincorporated back into the accumulating reef structure. This proportion was calculated as the sum of 50% of the parrotfish-derived sediment (as a highly mobile bioeroder which defecates randomly over the reef), as well as all sediment produced by urchins and by macroborer erosion. To keep our estimates conservative we worked on the assumption that only 50% of this bioerosional sediment yield is actually incorporated back into the reef (based on data from Hubbard[31]), and excluded any sediment generation by other benthic sediment producers (e.g *Halimeda* – although this calcareous green algae was extremely rare within our survey sites). Finally, we made an allowance for variations in the porosity of the accumulating reef framework as follows: 30% for head and massive coral dominated assemblages, 70% for branched and tabular dominated assemblages, and 50% for mixed coral assemblages (based on data in Kinsey & Hopley[32]). A loss factor to account for natural framework removal through physical processes was also included based on the data of Morgan and Kench[33], such that we

assumed that 20% of the annual framework produced was removed from more sheltered reef settings, and 50% from exposed settings.

To explore the accretion potential of the Chagos reefs in relation to sea level we compared our potential accretion rate estimates to both measured recent past and future projected sea-level rise rates. Recent sea-level trends around Chagos, based on tide-gauge records, are difficult to precisely constrain due to an apparent tide-gauge offset in the Diego Garcia record around 2002 (ref. 34). However, research that has integrated these records with satellite altimetry data suggests rise rates of ~2.2 mm yr^{-1} around Diego Garcia and 1.7 mm yr^{-1} around Peros Banhos and Salomon between 1993 to 2011 (ref. 34). These rates are above those reported (~1 mm yr^{-1}) from the central Indian Ocean region over the period 1950-2000 (ref. 35), but similar to those reported for Diego Garcia (~1.75 mm yr^{-1}) over the period 1950-2009 (ref. 36). However, a defining feature of Indian Ocean sea-level trends over time, and certainly over recent decades, is one of significant intra- and inter-annual variability, in part driven by the influence of the Indian Ocean Dipole (IOD). This causes marked variations in sea-surface temperatures and wind regimes across the region, and drives considerable cross-basin changes in sea-level. Caution is thus needed in interpreting long-term trends from the relatively short term datasets presently available. Whilst Dunne[34] argue that because of such inter-annual variability the long-term regional trend is not significantly different from zero (2.22 ± 1.80 SE mm yr^{-1} (ref. 34), it is perhaps more appropriate to conservatively assume that the local rate of rise over the last half century or so has probably not exceeded the global average of ~1.7 mm yr^{-1} (ref. 37) and ~2.2 mm yr^{-1} as measured over the last ~20 years in Chagos[34]. To compare contemporary reef accretion potential to future sea level rise trajectories we used the IPCC AR5 report projections for the period 2081-2100 (ref. 37), but also accounting for the impacts of future wind-stress[38] .

References:

1. Graham, N. A. J., Pratchett, M. S., McClanahan, T. R. & Wilson, S. K. in *Coral Reefs of the United Kingdom Overseas Territories SE - 19* (ed. Sheppard, C. R. C.) **4,** 253–270 (Springer Netherlands, 2013).
2. Chollett, I. & Mumby, P. J. Predicting the distribution of *Montastraea* reefs using wave exposure. *Coral Reefs* **31,** 493–503 (2012).
3. Graham, N. A. J., Jennings, S., MacNeil, M. A., Mouillot, D. & Wilson, S. K. Predicting climate-driven regime shifts versus rebound potential in coral reefs. *Nature* **518**, 94-97 (2015).
4. Rohweder, J. Rogala, J.T., Johnson, B.L., Anderson, D., Clark, S., Chamberlin, F., Potter, D., & Runyon, K. Application of wind fetch and wave models for habitat rehabilitation and enhancement projects – 2012 update (2012) http://www.umesc.usgs.gov/management/dss/wind_fetch_wave_models_2012update.html
5. U.S. Army Corps of Engineers. Shore Protection Manual, Coastal Engineering Research Center, Fort Belvoir, Virginia (1984).
6. Andréfouët, S. *et al.* Global assessment of modern coral reef extent and diversity for regional science and management applications: a view from space. in *Proceedings of the 10th International Coral Reef Symposium, Okinawa, Japan, 28 June-32nd July 2004* (eds. Suzuki, Y. et al.) (Japanese Coral Reef Society, 2006).
7. Hill, N. A. *et al.* Quantifying wave exposure in shallow temperate reef systems: Applicability of fetch models for predicting algal biodiversity. *Mar. Ecol. Prog. Ser.* **417,** 83–95 (2010)
8. Perry, C. T. *et al.* Estimating rates of biologically driven coral reef framework production and erosion: A new census-based carbonate budget methodology and applications to the reefs of Bonaire. *Coral Reefs* **31,** 853–868 (2012).
9. Januchowski-Hartley, F.A., McClanahan, T.R., Cossa, D., Perry, C.T. (in prep.) Isolation and community composition drive reef growth in East Arica.
10. Conand, C., Chabanet, P., Cuet, P., & Letourneur, Y. The carbonate budget of a fringing reef in La Reunion Island (Indian Ocean): sea urchin and fish bioerosion and net calcification. In *Proceedings of the 8th International Coral Reef Symposium* (eds. Lessios, H. A., & Macintyre, I. G., Vol. 1, Smithsonian Tropical Research Institute, Panama pp. 953-958 1987).
11. Glynn, P., Wellington, G. & Birkeland, C. Coral reef growth in the Galapagos: limitation by sea urchins. *Science* **203,** 47–49 (1979).
12. Scoffin, T. P. *et al.* Calcium-carbonate budget of a fringing-reef on the west-coast of Barbados. 2. Erosion, sediments and internal structure. *Bull. Mar. Sci.*, **30**, 475-508. (1980)

13. Griffin, S. P., García, R. P. & Weil, E. Bioerosion in coral reef communities in southwest Puerto Rico by the sea urchin *Echinometra viridis*. *Mar. Biol.* **143,** 79–84 (2003).
14. Russo, A.R. Bioerosion by two rock boring echinoids (*Echinometra mathaei* and *Echinostrephus aciculatus*) on Enewetak Atoll, Marshall Islands. *J. Mar. Res.* **38**, 99-110 (1980).
15. Downing, N. & El-Zahr, C. Gut evacuation and filling rates in the rock-boring sea urchin, *Echinometra mathaei*. *Bull. Mar. Sci.* **41,** 579–584 (1987).
16. McClanahan, T. R. & Mwashote, B. M. Changes in Kenian coral reef community structure and function due to exploitation. *Hydrobiologia* **166,** 269–276 (1988).
17. Bak, R. Patterns of echinoid bioerosion in two Pacific coral reef lagoons. *Mar. Ecol. Prog. Ser.* **66,** 267–272 (1990).
18. Mokady, O., Lazar, B. & Loya, Y. Echinoid bioerosion as a major structuring force of red sea coral reefs. *Biol. Bull.* **190,** 367–372 (1996).
19. Mills, S. C., Peyrot-Clausade, M. & France Fontaine, M. Ingestion and transformation of algal turf by *Echinometra mathaei* on Tiahura fringing reef (French Polynesia). *J. Exp. Mar. Bio. Ecol.* **254,** 71–84 (2000).
20. Carreiro-Silva, M. & McClanahan, T. R. Echinoid bioerosion and herbivory on Kenyan coral reefs: The role of protection from fishing. *J. Exp. Mar. Bio. Ecol.* **262,** 133–153 (2001).
21. Herrera-Escalante, T., López-Pérez, R. a. & Leyte-Morales, G. E. Bioerosion caused by the sea urchin *Diadema mexicanum* (Echinodermata: Echinoidea) at Bahías de Huatulco, Western Mexico. *Rev. Biol. Trop.* **53 Suppl 3,** 263–273 (2005).
22. Graham, N. A. J. & Mcclanahan, T. R. The Last Call for Marine Wilderness? *Bioscience* **63,** 397–402 (2013).
23. Letourneur, Y. Length-weight relationship of some marine fish species in Reunion Island, Indian Ocean. *Naga*, **21**, 37-39 (1998).
24. Froese, R. & Pauly, D. FishBase (www.fishbase.org). World wide web electronic publication (2012)
25. Bellwood, D. Direct estimate of bioerosion by two parrotfish species, *Chlorurus gibbus* and *C. sordidus*, on the Great Barrier Reef, Australia. *Mar. Biol.* 419–429 (1995).
26. Ong, L. & Holland, K. N. Bioerosion of coral reefs by two Hawaiian parrotfishes: species, size differences and fishery implications. *Mar. Biol.* **157,** 1313–1323 (2010).
27. Lokrantz, J., Nyström, M., Thyresson, M. & Johansson, C. The non-linear relationship between body size and function in parrotfishes. *Coral Reefs* **27,** 967–974 (2008).
28. Bellwood, D. R. & Choat, J. H. A functional analysis of grazing in parrotfishes (family Scaridae): the ecological implications. *Environ. Biol. Fishes* **28,** 189–214 (1990).
29. Bruggemann, J., van Kessel, A., van Rooij, J. & Breeman, A. Bioerosion and sediment ingestion by the Caribbean parrotfish *Scarus vetula* and *Sparisoma viride*: implications of fish size, feeding mode and habitat use. *Mar. Ecol. Prog. Ser.* **134,** 59–71 (1996).
30. Perry, C. T. *et al.* Caribbean-wide decline in carbonate production threatens coral reef growth. *Nat. Commun.* **4,** 1402 (2013).
31. Hubbard, D. K. Depth and species-related patterns of Holocene reef accretion in the Caribbean and western Atlantic: a critical assessment of existing models. *Spec. Publ. Int. Assoc. Sedimentol*. **40**, 1–18 (2008).
32. Kinsey, D.W. & Hopley, D. The significance of coral reefs as global carbon sink-response to greenhouse. *Palaeogeogr. Palaeoclimatol. Palaeoecol.* **89**, 363–377 (1991).
33. Morgan KM & Kench PS A detrital sediment budget of a Maldivian reef platform. *Geomorphology* **222**, 122–131 (2014).
34. Dunne, R. P., Barbosa, S. M. & Woodworth, P. L. Contemporary sea level in the Chagos Archipelago, central Indian Ocean. *Global and Planetary Change*. 82-83: 25-37.
35. Church, J.A., White, N.J. & Hunter, J.R. Sea-level rise at tropical Pacific and Indian Ocean islands. *Global and Planetary Change* **53**, 155–168 (2006).
36. Palanisamya, H. *et al.* Regional sea level variability, total relative sea level rise and its impacts on islands and coastal zones of Indian Ocean over the last sixty years. *Global and Planetary Change* **116**, 54–67 (2014).
37. Church, J.A. *et al.* Sea Level Change. In: *Climate Change 2013: The Physical Science Basis. Contribution of Working Group I to the Fifth Assessment Report of the Intergovernmental Panel on Climate Change* [Stocker, T.F., D. Qin, G.-K. Plattner, M. Tignor, S.K. Allen, J. Boschung, A. Nauels, Y. Xia, V. Bex and P.M. Midgley (eds.)]. Cambridge University Press, Cambridge, United Kingdom and New York, NY, USA (2013).
37. Timmermann, A., S. McGregor, & Jin, F. F. Wind effects on past and future regional sea level trends in the southern Indo-Pacific, *J. Clim.* **23**, 4429–4437 (2010)

Supplementary Table S1

Site	% *Acropora*	% *Porites*	% *Pocillop.*	% other corals	Cover cover %	Gross G	Erosion G	Net G	Accretion rate (mm yr^{-1})	Exposure (j m^{-3})
Diego Garcia										
Cannon Point S 07°15'27.3"; E 072°22'14.8"	18	11	23	48	16.5	2.72	2.12	0.60	1.32	673
Middle Island S 07°13'35.3"; E 072°24'28.02	37	31	9	23	36.4	8.04	4.00	4.04	1.51	678
Barton Point S 07°14'00.3"; E 072°26'23.9"	36	33	3	28	42.9	9.77	2.97	6.79	1.64	1065
East Island S 07°13'25.0"; E 072°25'16.3"	15	27	22	36	10.6	2.02	1.45	0.57	1.27	1050
Horsborough Bay S 07°13'33.9"; E 072°24'29.1"	6	20	6	68	27.7	6.06	1.67	4.74	1.7	1005
Peros Banhos										
Ile Poule S 05°23'52.2"; E 071°44'57.6"	59	18	3	20	40.9	11.71	3.75	8.23	2.29	797
Ile Gabrielle S 05°25'15.0"; E 071°44'50.0"	56	15	3	26	30.5	7.09	2.83	4.31	2.18	884
Ile Diamante S 05°14'46.8"; E 071°46'10.1"	29	24	5	42	35.3	7.46	2.59	4.87	2.04	652
Ile de la Passe S 05°14'14.8"; E 071°48'57.4"	48	23	4	25	37.1	10.34	3.36	6.98	2.48	702
Ile Fouquet S 05°27'40.3"; E 071°46'23.5"	16	48	16	20	24.7	7.55	3.36	4.19	2.05	1265
Petite Coquillage S 05°20'22.9"; E 071°58'40.0"	15	54	9	22	39.7	10.15	7.44	2.7	1.95	1405
Grand Coquillage S 05°22'20.9"; E 071°58'31.2"	17	60	6	17	34.9	11.42	1.64	9.76	2.28	1389
Salomon										
Ile Anglaise – south S 05°20'22.7"; E 072°12'49.1"	75	12	2	11	24.3	7.81	3.93	3.87	2.57	510
Ile Anglaise – middle S 05°19'45.0"; E 072°13'10.5"	48	23	7	22	22.1	7.88	3.96	3.91	2.71	514
Ile Anglaise – north S 05°18'58.7"; E 072°13'32.1"	31	49	7	13	28.1	9.57	1.80	7.77	2.38	623
Ile de Passe S 05°14'14.8"; E 071°48'57.4"	56	22	10	12	33.1	9.16	4.04	5.12	2.32	780
Ile Takamaka S 05°19'80.0"; E 072°16'50.0"	10	44	32	14	6.6	1.64	1.52	0.12	1.3	1690
Ile du Sel S 05°21'37.4"; E 072°13'36.4"	12	45	9	34	13.6	3.75	3.50	0.24	1.81	1404
Blenheim										
Blenheim, west side S 05°12'11.4"; E 072°27'16.7"	52	2	20	26	30.4	7.68	3.64	4.04	1.91	688
Gt Chagos Bank										
Nelson, north S 05°40'46.9"; E 072°18'59.7"	0	45	10	45	3.6	1.86	6.88	-5.03	2.27	545
Eagle - northern end S 06°10'26.4"; E 071°19'60.0"	24	64	4	8	21.3	4.92	2.26	2.66	1.65	795
Eagle - southern end S 06°12'10.1"; E 071°18'44.6"	6	57	7	30	19.3	5.55	3.28	2.26	1.91	761
Eagle - middle site S 06°11'18.0"; E 071°19'10.5"	16	54	7	23	12.9	3.27	4.08	-0.81	1.5	770
Danger Island S 06°23'30.0"; E 071°14'40.0"	13	38	21	28	10.1	3.72	3.98	-0.26	1.95	591
Middle Brother S 06°09'21.6"; E 071°30'40.0"	35	32	1	32	34.6	8.06	2.60	5.47	2.04	1193
South Brother - west end S 06°10'25.3"; E 071°32'18.3"	65	14	3	18	40.7	10.07	5.46	4.59	2.11	1212

South Brother - east end S 06°10'30.4"; E 071°32'34.0"	41	21	7	31	43.4	10.65	3.87	6.78	1.98	1288
Egmont										
Egmont S 06°38'44.5"; E 071°22'12.0"	41	16	4	39	29.9	6.88	2.06	4.81	1.9	1133